Food and Chemical Toxicology 60 (2013) 360–368

Contents lists available at ScienceDirect

Food and Chemical Toxicology

journal homepage: www.elsevier.com/locate/foodchemtox

Brief communication

Silibinin meglumine, a water-soluble form of milk thistle silymarin, is an orally active anti-cancer agent that impedes the epithelial-to-mesenchymal transition (EMT) in EGFR-mutant non-small-cell lung carcinoma cells

Sílvia Cufí [a,b,1], Rosa Bonavia [c,1], Alejandro Vazquez-Martin [a,b,1], Bruna Corominas-Faja [a,b], Cristina Oliveras-Ferraros [a,b], Elisabet Cuyàs [a,b], Begoña Martin-Castillo [b,e], Enrique Barrajón-Catalán [f,g], Joana Visa [d], Antonio Segura-Carretero [h], Joaquim Bosch-Barrera [b,d], Jorge Joven [i], Vicente Micol [f,g,*], Javier A. Menendez [a,b,*]

[a] Metabolism & Cancer Group, Translational Research Laboratory, Catalan Institute of Oncology, Girona, Catalonia, Spain
[b] Girona Biomedical Research Institute (IDIBGi), Girona, Catalonia, Spain
[c] Animal Care Facility, Institut d'Investigació Biomèdica de Bellvitge (IDIBELL), L'Hospitalet de Llobregat, Barcelona, Catalonia, Spain
[d] Medical Oncology, Catalan Institute of Oncology, Girona, Catalonia, Spain
[e] Unit of Clinical Research, Catalan Institute of Oncology, Girona, Catalonia, Spain
[f] Molecular and Cellular Biology Institute (IBMC), Miguel Hernández University, Elche, Alicante, Spain
[g] Monteloeder, Inc., Elche, Alicante, Spain
[h] Department of Analytical Chemistry, Faculty of Sciences, University of Granada, Granada, Spain
[i] Unitat de Recerca Biomèdica (URB-CRB), Institut d'Investigació Sanitaria Pere i Virgili (IISPV), Universitat Rovira i Virgili, Reus, Catalonia, Spain

ARTICLE INFO

Article history:
Received 23 May 2013
Accepted 22 July 2013
Available online 1 August 2013

Keywords:
Milk thistle
Silibinin
Silibinin meglumine
Lung cancer
Gefitinib
EMT

ABSTRACT

Silibinin is the primary active constituent of a crude extract (silymarin) from milk thistle plant (*Silybum marianum*) seeds. We explored the ability of an oral milk thistle extract formulation that was enriched with a water-soluble form of silibinin complexed with the amino-sugar meglumine to inhibit the growth of non-small-cell lung carcinoma (NSCLC) mouse xenografts. As a single agent, oral silibinin meglumine notably decreased the overall volumes of NSCLC tumors as efficiently as did the EGFR tyrosine kinase inhibitor (TKI) gefitinib. Concurrent treatment with silibinin meglumine impeded the regrowth of gefitinib-unresponsive tumors, resulting in drastic tumor growth prevention. Because the epithelial-to-mesenchymal transition (EMT) is required by a multiplicity of mechanisms of resistance to EGFR TKIs, we evaluated the ability of silibinin meglumine to impede the EMT *in vitro* and *in vivo*. Silibinin-meglumine efficiently prevented the loss of markers associated with a polarized epithelial phenotype as well as the *de novo* synthesis of proteins associated with the mesenchymal morphology of transitioning cells. Our current findings with this non-toxic, orally active, and water-soluble silibinin formulation might facilitate the design of clinical trials to test the administration of silibinin meglumine-containing injections, granules, or beverages in combination with EGFR TKIs in patients with EGFR-mutated NSCLC.

© 2013 Elsevier Ltd. All rights reserved.

1. Introduction

Silybum marianum (L.) Gaertn. (*Carduus marianus* L., Asteraceae; milk thistle) seeds have been used since ancient times to treat a large variety of liver and gallbladder disorders. Theoprastus (fourth century B.C.), Dioskurides and Plinius (first century A.D.) were the first to report the medicinal benefits of this plant. The use of *Silybum* extract to treat liver diseases such as cirrhosis, hepatitis, alcoholic liver disease and toxin exposure has been well documented for more than 40 years (de Groot and Rauen, 1998; Flora et al., 1998; Fraschini et al., 2002; Halbach and Trost, 1974). Silymarin is the accepted name for the *S. marianum* extract, which is obtained

* Corresponding authors. Addresses: Instituto de Biología Molecular y Celular (IBMC), Universidad Miguel Hernández, Avenida de la Universidad s/n, E-03202 Elche, Alicante, Spain. Tel.: +34 966 658430; fax: +34 966 658758 (V. Micol), Catalan Institute of Oncology, Girona (ICO-Girona) Hospital Dr. Josep Trueta de Girona, Ctra, França s/n, E-17007 Girona, Catalonia, Spain. Tel.: +34 972 225834x2553; fax: +34 972 217344 (J.A. Menendez).
E-mail addresses: vmicol@umh.es (V. Micol), jmenendez@iconcologia.net, jmenendez@idibgi.org, jbosch@iconcologia.net (J.A. Menendez).
[1] These authors contributed equally to this work.

0278-6915/$ - see front matter © 2013 Elsevier Ltd. All rights reserved.
http://dx.doi.org/10.1016/j.fct.2013.07.063

through organic solvent extraction and contains a high fraction of flavonolignan monomers (e.g., silybin, isosilybin, silychristin, and silydianin) and a smaller fraction of polymeric and oxidized polyphenolic components. Silybin or silibinin (CAS No. 22888-70-6), a 1:1 mixture of the diasteroisomers silybin A and silybin B, is the major compound in this extract (Lee and Liu, 2003).

Silymarin has very poor bioavailability due to the poor water solubility (<0.04 mg/mL) of its flavonolignan structure. This fact considerably limits clinical applications and therapeutic efficiency of silymarin; accordingly, many different pharmaceutical preparations have been developed in the last two decades to increase its bioavailability (Javed et al., 2011; Pei et al., 2009). Some of the preparations intended to improve silymarin oral bioavailability are based on physical blends of excipients (e.g., dextrin, starch, sucrose) and silymarin at certain particle sizes, which are then administered as capsules, tablets, or granules (Chinese-State-Drug-Administration, 2002). Other more sophisticated preparations have used β-cyclodextrin inclusions (Liu and Yan, 1996) or solid PVP, PEG, urea or poloaxamer-containing dispersions (Tang et al., 2001), leading to the discovery that PVP solid dispersions have the highest solubilization efficiency among these carriers. Silymarin liposomes, which were designed to target hepatic lesions by taking the advantage of passive targeting into the liver, have demonstrated high encapsulation efficiency and enhanced gastrointestinal absorption when compared to silymarin (Xiao et al., 2005; Yu et al., 2003). Silymarin has also been complexed with phosphatidylcholine in a formulation that was initially named silipide (IdB 1016) or Siliphos® (Indena, Italy). Several studies have indicated the improved absorption and bioavailability of this formulation in rats compared to those of silymarin (Morazzoni et al., 1993). Several silybin metabolites were identified in plasma samples from colorectal cancer patients who received daily doses of 1.45 g/day for seven days (Kidd, 2009); however, the silybin plasma concentrations failed to reach levels above 4 μmol/L, which hardly justify most of the observed effects in cultured human cancer cell models. Silymarin nanoparticles of 150 nm in size, which were obtained via solution-enhanced dispersion with a supercritical fluid technique, have shown improved bioavailability in rats (e.g., 2.5-fold) when compared to particles of 1000 nm in size (He et al., 2005). A comparative review of the different strategies to improve silymarin bioavailability has recently been published (Javed et al., 2011). Although the results are hardly comparable due to assay condition variability, silybin glycoside formation was shown to enhance bioavailability up to 30-fold when compared with regular silymarin, followed by cyclodextrin complexation (20-fold), phospholipid complexation (10-fold), and solid dispersions (5-fold).

Silymarin has been successfully solubilized in water through a meglumine salt preparation. This orally administered silymarin formulation demonstrated improved efficacy against cisplatin-induced renal injuries in rats when compared to silymarin in tablet form (Lu et al., 1999). A water-soluble formulation of silibinin, complexed with the excipient amino-sugar meglumine (Fig. 1), can also be incorporated into silica nanoparticles that permit a sustained silybin release system (Cao et al., 2012). Because a water-soluble silibinin formulation is crucial for target preparations as it will enable new breakthroughs in silibinin meglumine-containing injection, granule, or beverage formation, we have preclinically explored for the first time whether silibinin meglumine might represent an inexpensive adjuvant strategy for orally administered silymarin in cancer patients. Because silibinin has demonstrated strong anti-cancer efficacy against non-small-cell lung carcinoma (NSCLC) cells in both culture and nude mice (Mateen et al., 2010, 2012; Rho et al., 2010), we decided to compare the ability of an orally administered silibinin meglumine (30% w/w)-enriched milk thistle extract to inhibit the growth of NSCLC mouse xenografts that harbor the ΔE746A750 activating EGFR mutation with that of the EGFR tyrosine kinase inhibitor (TKI) gefitinib, a first-line treatment for EGFR mutation-positive advanced NSCLC.

2. Materials and methods

2.1. Materials

The EGFR (HER1)-Tyrosine Kinase Inhibitor (TKI) gefitinib (ZD1839; Iressa®) was kindly provided by AstraZeneca PLC (London, UK). Recombinant human (carrier-free) TGFβ1 was purchased from R&D Systems Inc. (Minneapolis, MA, USA).

2.2. High-performance liquid chromatography-electrospray tandem mass spectrometry (HPLC–ESI-MS/MS)

The milk thistle extract composition was analyzed and quantified by HPLC–DAD-ESI-MS/MS on an Agilent LC 1100 series (Agilent Technologies, Inc., Palo Alto, CA, USA). The instrument was controlled by ChemStation software (Agilent Technologies, Inc.) and equipped with a pump, auto-sampler, column oven, and UV–vis diode array detector. The HPLC instrument was coupled to an Esquire 3000+(Bruker Daltonics, GmbH, Germany) mass spectrometer equipped with an ESI source and ion-trap mass analyzer, which was operated by Esquire control and data analysis software. The extract was separated by a gradient method that used H_3PO_4:MeOH:water (0.05:20:79.95) as solvent A and H_3PO_4:MeOH:water (0.05:79.95:20) as solvent B. The gradient included 15% B, 15% B at 2 min, 45% at 20 min, 45% at 40 min, 15% at 41 min, and a final re-equilibration at 15% B until 55 min. The flow rate was 1 mL/min. An Alltech Prevail C18 3 μm, 150 × 4.6-mm column was used for the separation. The diode-array detection was set at 288 nm. The ESI source was processed in a negative mode to generate ions under the following conditions: desolvation temperature at 360 °C and vaporizer temperature at 400 °C, and the dry gas (nitrogen) and nebulizer were set at 12 L min^{-1} and 70 psi, respectively. The MS data were collected from the full-scan mass spectra at 50–1100 *m/z*, using 200 ms to collect the ions in the trap. The compounds were identified by HPLC–DAD analysis. The retention time, UV spectra, and MS/MS data of the sample peaks were compared to data reported in the literature (Brinda et al., 2012; Calani et al., 2012; Kuki et al., 2012; Wang et al., 2010). Quantitation of the main flavonolignan compounds was performed using ChemStation for LC 3D software (Agilent Technologies Life Sciences and Chemical Analysis, Waldbronn, Germany), and the silibinin equivalents were determined with silibinin standards (Sigma–Aldrich).

2.3. Cell culture

PC-9 NSCLC-derived cells that expressed the EGFR exon 19 deletion mutation (*ΔE746-A750*) were obtained from the IBL cell bank (Gunma, Japan). PC-9 cells were routinely grown in Dulbecco's modified Eagle's medium (DMEM, Gibco® Cell Culture Systems) with 10% heat-inactivated fetal bovine serum (FBS, Bio-Whittaker, Inc.), 1% L-glutamine, 1% sodium pyruvate, 50 U/mL of penicillin, and 50 μg/mL of streptomycin. The cells were maintained at 37 °C in a humidified atmosphere with 5% CO_2.

2.4. Tumor cell implantation experiments

A total of 20 non-obese diabetic/severe combined immunodeficiency (NOD/SCID) mice, purchased from Charles River Laboratories, were subcutaneously inoculated with 5×10^6/100 μl PC-9 cells. Subcutaneous tumor growth was monitored daily; when the solid tumors reached a volume of 100 mm^3, the animals were randomly assigned to groups of 5 animals each. These groups were treated with the vehicle control, gefitinib (100 mg/kg, 5 days a week), silibinin meglumine (100 mg/kg, 5 days a week), or gefitinib plus silibinin-meglumine. All drugs were administered *via* oral gavage. The mice were weighed once per week after dosing. The tumor sizes were measured daily with electronic calipers, and the tumor volumes were calculated with the following formula: volume (mm^3) = length × $width^2$ × 0.5. After 35 days of oral treatment, the mice were euthanized by cervical dislocation and the tumors were collected. Tumor growth curves were obtained by plotting the median volume values on the *y*-axis against time (expressed as days after initiation of therapy) on the *x*-axis. The experiments were approved by the Institutional Animal Care and Use Committee (IACUC) of the Institut d'Investigació Biomèdica de Bellvitge (IDIBELL; Animal Use Protocol #6302 authorized by the Animal Experimental Commission of the Catalan Government, Barcelona, Spain).

2.5. Quantitative real-time polymerase chain reaction (qRT-PCR)

For the purification of total RNA from the tumor tissues, we used Qiagen miRNeasy Mini kits (Cat. No. 217004) and QIAshredder columns, according to the manufacturer's instructions. One microgram of total RNA was reverse-transcribed to

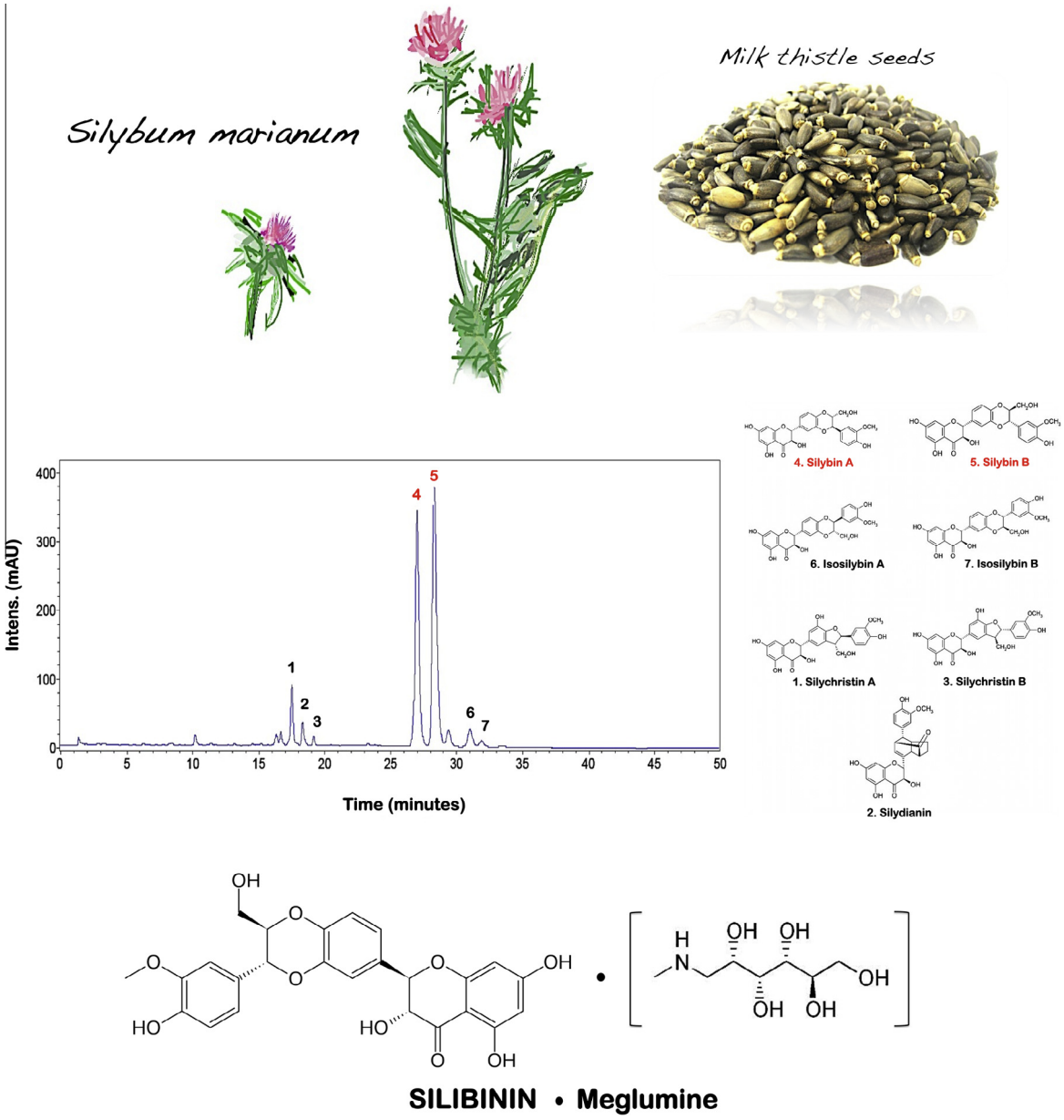

Fig. 1. HPLC chromatogram of milk thistle extract with 30% (w/w) of water-soluble silibinin meglumine at 288 nm. Compounds are identified by number as follows: silychristin A (1), silydianin (2), silychristin B (3), silybin A (4), silybin B (5), isosilybin A (6) and isosilybin B (7).

cDNA using the Reaction Ready™ First Strand cDNA Synthesis Kit (SABiosciences) and applied to a customized PCR array in a 96-well format. The PCR array contained the following panel of genes: *TWIST*, *SNAI2* (*SLUG*), *VIM*, *CDH1*, and *CDH2*. The arrays were processed according to the SABiosciences RT-PCR manual and analyzed using an Applied Biosystems 7500 Fast Real-Time PCR System with an automated baseline and threshold cycle detection. The data were interpreted using a web-based PCR array analysis tool from SABiosciences.

2.6. Immunofluorescence staining and high-content confocal imaging

For imaging, the cells were seeded at a density of approximately 5,000 cells/well in 96-well clear-bottom tissue culture plates (Becton Dickinson Biosciences; San Jose, CA, USA) that were optimized for automated imaging applications. Triton® X-100 permeabilization and blocking, primary antibody staining, secondary antibody staining with Alexa Fluor® 488/594-conjugated goat anti-rabbit/mouse IgGs (Invitrogen-Molecular Probes, Eugene, OR, USA), and Hoechst 33258 counterstaining (Invitrogen) were performed according to protocols from BD Biosciences. The images were captured in different channels for Alexa Fluor® 488 (pseudocolored green), Alexa Fluor® 594 (pseudocolored red), and Hoechst 33258 (pseudocolored blue) staining on a BD Pathway™ 855 Bioimager System (Becton Dickinson Biosciences) with 20× or 40× objectives (NA 075, Olympus). Merged images were obtained with BD Attovision™ software according to the recommended assay procedure.

2.7. Wound-healing motility assays

PC-9 cells were seeded onto six-well dishes at 1×10^5 per well. A single scratch wound was creased using a p10 micropipette tip into confluent cells. Cells were washed twice with PBS to remove cell debris, supplemented with regular growth medium in the absence or presence of silibinin meglumine-enriched milk thistle extract, TGFβ1 or TGFβ1 + silibinin meglumine-enriched milk thistle extract, and monitored. Images were captured by phase-contrast microscopy at 0, 24, and 48 h after wounding.

3. Results

All the identified flavonolignan isomers in the milk thistle extract, including silychristin A, silychristin B, silydianin, silybin A, silybin B, isosilybin A, and isosilybin B, had base peaks at *m/z*

481 that corresponded to the negatively charged molecular ion ($[M-H]^-$) and a main fragment ion at *m/z* 125 (MS/MS) that was derived from A-ring fission, as previously reported (Calani et al., 2012). Quantification of the water-soluble silymarin extract flavonolignans with a silibinin A + B standard revealed a total flavonolignan content of 32.93% (*w/w*; silychristin A, silychristin B, silydianin, silybin A, silybin B, isosilybin A, and isosilybin B) and a total silibinin content of 29.96% (*w/w*; silybin A, silybin B, isosilybin A, and isosilybin B).

3.1. Oral administration of silibinin meglumine delays tumor growth in EGFR-mutant NSCLC mouse xenografts and impedes EMT in vivo

The effects of a systemic silibinin meglumine treatment on tumor growth were studied in a xenograft animal model of PC-9 tumors that contained the EGFR TKI-sensitizing Δ*E746-A750* deletion mutation in exon 19 of the *EGFR* gene. When the tumor volumes reached approximately 100 mm^3 (as measured with calipers), the mice were randomly allocated into four groups of 5 animals each. The groups received gefitinib, silibinin meglumine, gefitinib + silibinin meglumine or vehicles by oral gavage. The mice in each group were followed and their tumors measured during a 35-day treatment period; the tumor volumes were calculated for each mouse at each time point. Fig. 2A (*left panel*) shows the tumor growth rate in the three treatment groups; the data are plotted as the mean tumor volume in each group over time. The tumor volumes in the gefitinib-treated animals at all time points were smaller than the initial volume, and this decrease in volume became statistically significant at day 14. When compared to the animals in the vehicle-treated group (mean tumor volume: 327 ± 45 mm^3), 5 weeks of oral gavage gefitinib treatment for 5 days/week at 100 mg/kg body weight by oral gavage significantly prevented tumor growth in animals with PC-9 xenografts (mean tumor volume: 168 ± 40 mm^3). Five weeks of oral gavage silibinin meglumine treatment for 5 days/week at 100 mg/kg body weight was as efficient as the EGFR TKI gefitinib with regard to marked time-dependent xenograft growth prevention. Thus, compared to the mean xenograft tumor volume in the untreated control animals, daily oral gavage with silibinin meglumine resulted in a remarkable reduction in the mean tumor volume to 151 ± 39 mm^3.

The combined gefitinib and silibinin meglumine treatment reduced the PC-9 xenograft growth to tumor volumes as low as 96 ± 14 mm^3 during the same treatment period. These findings strongly suggest that the EGFR-mutant PC-9 xenografts were fully sensitized to the tumor growth inhibitory effects of gefitinib in the presence of silibinin meglumine. This was reflected by the percentage of tumor growth inhibition, which was calculated as 1-treated/control volume ratios (1-T/C) (Fig. 2A, *right panel*). The inhibitory effect of gefitinib reached a maximum after 4 weeks (62%) but decreased toward the end of the treatment to the lower levels of activity that were observed during the first weeks of treatment (~50%). The anti-tumor activity profile of the single agent silibinin-meglumine was mostly equivalent to the inhibitory effect of single agent gefitinib, reaching a plateau of maximum activity after 3 weeks of treatment (~54%) and remaining constant until the end of the 5-week treatment schedule. Notably, the anti-tumor activity in the combined gefitinib and silibinin meglumine group increased

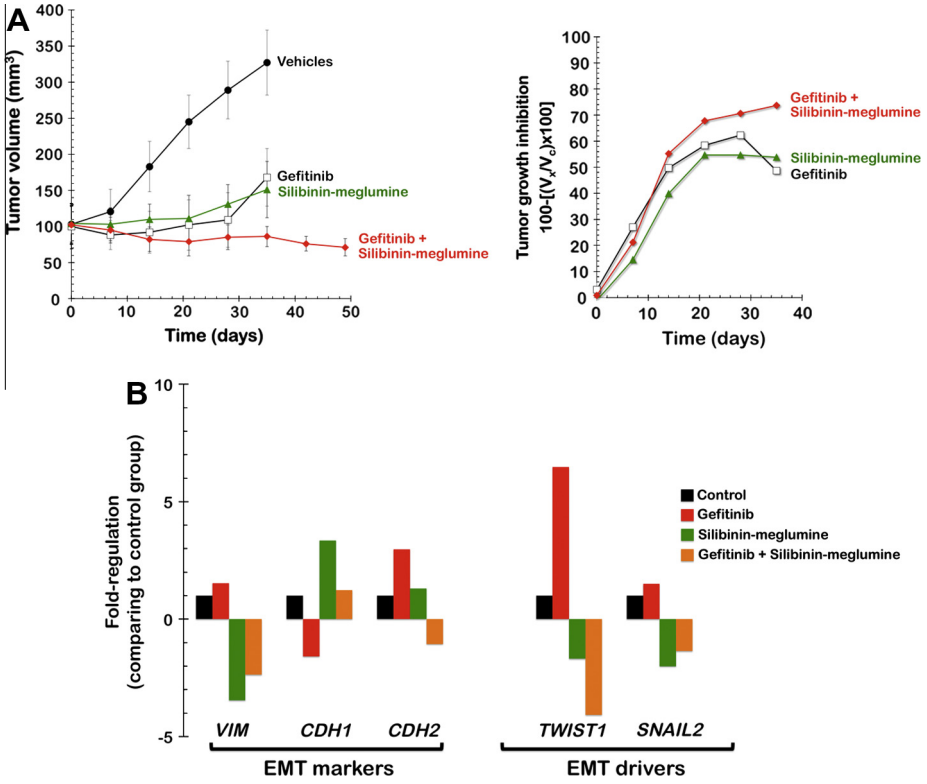

Fig. 2. Oral treatment of EGFR-mutant NSCLC xenograft-bearing animals with silibinin meglumine: Impact on the efficacy of the EGFR TKI gefitinib and in the mesenchymal phenotype *in vivo*. (A). *Left.* Shown are the mean tumor volumes (±SD) in PC-9 xenograft-bearing nude mice following oral gavage with gefitinib, silibinin meglumine or gefitinib *plus* silibinin meglumine for five weeks as specified. *Right.* Antitumor activity was calculated for individual tumors as the percentage of tumor growth inhibition, according to the following formula: $100-[(V_x/V_c) \times 100]$, where V_x is the tumor volume for treated mice and V_c is the tumor volume in the control group at a given *x* time. (B) Figure shows the greatest difference (by fold-change) in the mRNA relative expression of the mesenchymal markers *VIM*, *CDH1*, and *CDH2*, and the EMT-inducing transcription factors *TWIST1* and *SNAIL2*, all of which were found significantly regulated in PC-9 tumors following oral gavage with gefitinib, silibinin meglumine or gefitinib *plus* silibinin meglumine for five weeks as specified.

in a time-dependent manner, reaching a maximum of 74% after 35 days.

Emerging data has repeatedly implicated the epithelial-to-mesenchymal (EMT) phenomenon as a contributor to both innate and acquired resistance to EGFR TKIs (Bryant et al., 2012; Byers et al., 2013; Thomson et al., 2005; Chang et al., 2011; Chung et al., 2011; Coldren et al., 2006; Fuchs et al., 2008; Nurwidya et al., 2012; Suda et al., 2011; Yauch et al., 2005; Zhang et al., 2012, 2013); indeed, it is reasonable to suggest that the activation of an EMT genetic program is a core resistance mechanism that bypasses pharmacological EGFR pathway inhibition in NSCLC. As such, we hypothesized that silibinin meglumine might operate as a negative regulator of the EMT phenotype *in vivo*. After 35 days of oral treatment with gefitinib, silibinin meglumine, or gefitinib plus silibinin meglumine, tumors were collected and snap frozen for the isolation of total RNA. We then used a customized array for the quantitative of five mRNAs that are functionally associated with EMT and the reciprocal mesenchymal-to-epithelial transition (MET), namely the EMT markers *VIM* (vimentin), *CDH1* (E-cadherin), *CDH2* (N-cadherin), and the EMT-inducing transcriptional factors *TWIST1*, and *SNAI2 (SLUG)* (Fig. 2B). The results strongly suggested that PC-9 tumors treated with gefitinib experienced slight but significant changes in the mRNA expression of mesenchymal phenotype cell markers; gefitinib-treated tumors notably enhanced the relative mRNA expression of *TWIST1*, a recently confirmed determinant of the acquisition of a mesenchymal phenotype in *EGFR* mutated NSCLC (Nakashima et al., 2012; Pallier et al., 2012). Accordingly, gefitinib treatment notably increased the relative mRNA expression of *CDH2* (N-cadherin), a mesenchymal cadherin associated with EMT that has consistently been found to be up-regulated in most biopsies obtained from recurrent NSCLC patients that progressed on EGFR TKI-based therapies (Zhang et al., 2013). In contrast, five weeks of oral gavage silibinin meglumine treatment induced up-regulation of the relative mRNA expression of*CDH1* (E-cadherin) accompanied with down-regulation of *VIM* (vimentin); moreover, the concurrent treatment with silibinin meglumine drastically prevented the up-regulatory effects of gefitinib on *TWIST1* mRNA expression.

3.2. Silibinin meglumine impedes TGFβ-induced EMT in PC-9 NSCLC cells in vitro

We sought to determine whether silibinin meglumine could prevent TGFβ1 from activating an EMT protein signature, as defined by low E-cadherin and high vimentin expression levels, *in vitro*. Upon treatment with TGFβ1, Δ*E746-A750*-mutated PC-9 cells initially exhibited a typical epithelial-like morphology, but subsequently showed reductions in cell–cell contacts and gradually progressed to a spindle-shaped morphology. This was evident after a 24-h TGFβ1 treatment, and the cells continued to elongate at and beyond 48 h (Fig. 3A). The drastic TGFβ1-induced redefinitions of cell shape and morphology included the striking formation of long F-actin filament stress fibers, which was accompanied by the significant accumulation of cytoplasmic mesenchymal markers such as the intermediate filament vimentin. Remarkably, exogenous supplementation with silibinin meglumine largely impeded the ability of the TGFβ1-treated PC-9 cells to undergo a full EMT (Fig. 3A). After a 72-h incubation with TGFβ1, F-actin was mostly assembled into thick parallel bundles or actin stress fibers that traversed the ventral cell surface. In the presence of silibinin meglumine, filamentous actin was mostly organized into cortical bundles that were associated with cell–cell adhesions (Fig. 4). Additionally, silibinin meglumine impeded the ability of TGFβ1 to alter E-cadherin cycling between the cytoplasm and cell membrane that would promote its rapid internalization. Accordingly, a visible loss of cell–cell contacts, the rapid internalization of E-cadherin, and the significantly reduced re-expression of the mesenchymal-specific marker vimentin were observed in the presence of silibinin meglumine (Fig. 4). All these phenomena related to changes in the cell migratory behavior of PC-9 cells. *In vitro* scratch

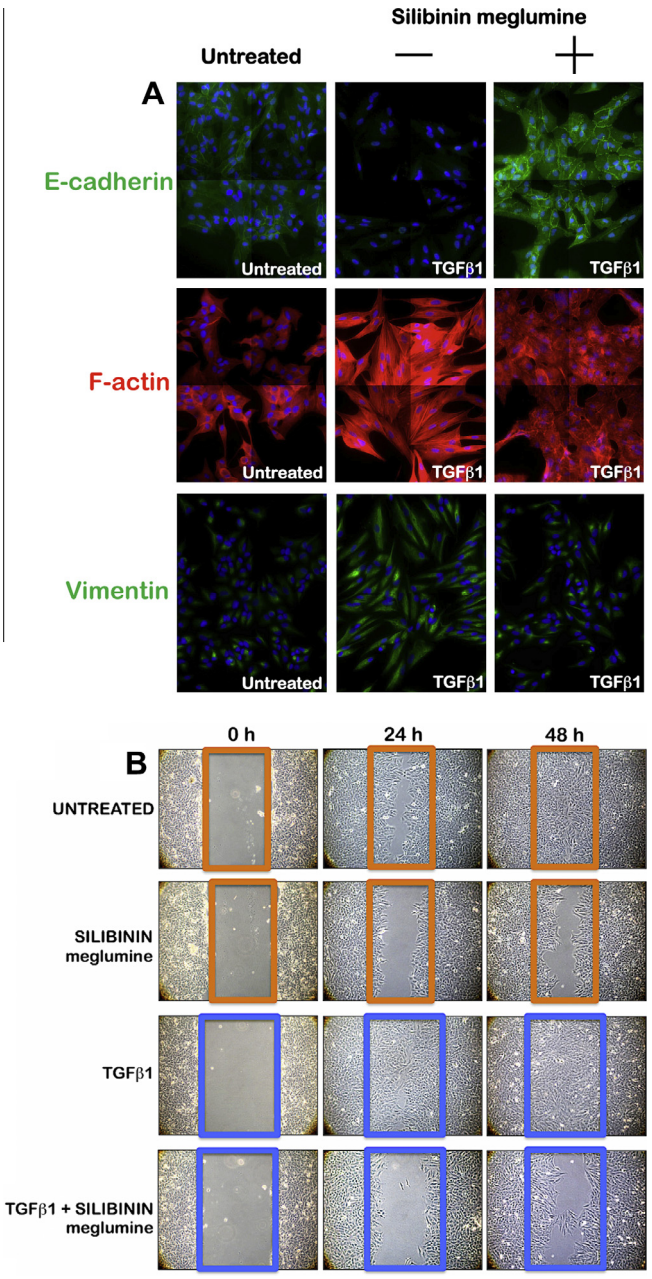

Fig. 3. Silibinin meglumine impedes TGFβ1-induced EMT and the migratogenic phenotype in PC-9 cells. A. PC-9 cells were grown to 75–80% confluence, serum-starved for 24 h, and then treated for 3 days with 10 ng/mL of TGFβ1 in the absence or presence of 100 μg/mL of silibinin meglumine. *Top panels.* After fixation and permeabilization, the subcellular distribution of F-actin, the epithelial marker E-cadherin, and of the mesenchymal-specific marker vimentin was assessed after staining with anti-F-actin, anti-E-cadherin, and anti-vimentin antibodies and Hoechst 33258 for nuclear counterstaining, as specified. Images show representative portions of the untreated-, TGFβ1-, silibinin meglumine-, or TGFβ1 + silibinin meglumine-treated PC-9 cells in montages of 4×4, which were captured in different channels for F-actin (*red*), E-cadherin (*green*), vimentin (*green*), and Hoechst 33258 (*blue*) with a 20x objective. Images were merged on a BD Pathway 855 Bioimager System with BD Attovision software. (B) Figure shows representative microphotographs of wound healing assays 0, 24, and 48 h after incisions of confluent PC-9 cells cultured in the absence or presence of silibinin meglumine (100 μg/mL), TGFβ1 (10 μg/mL), or TGFβ1 + silibinin meglumine as specified.

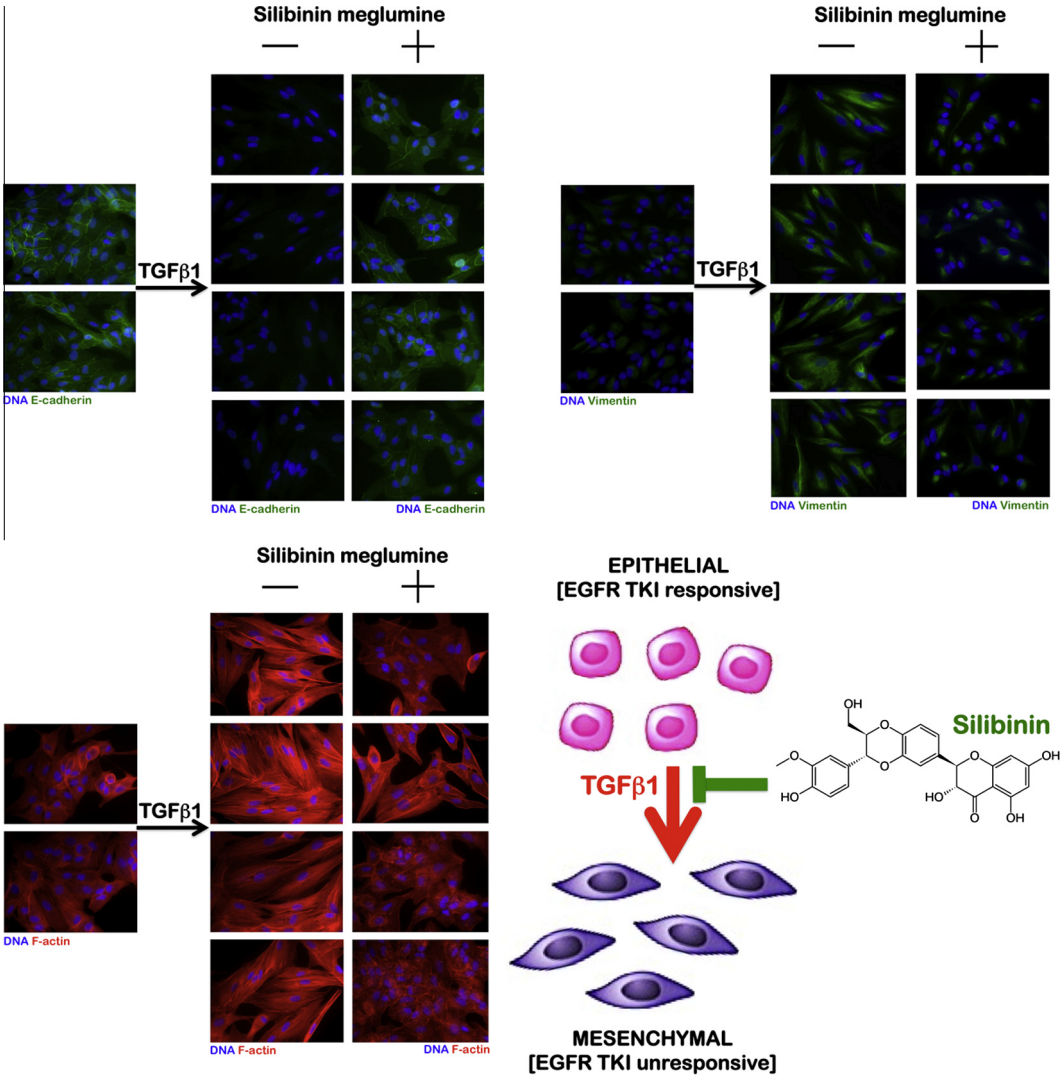

Fig. 4. Silibinin: A new strategy to target molecules that control the acquisition of an EGFR TKI-refractory mesenchymal-like phenotype by EGFR TKI-responsive epithelial NSCLC cells.

wound healing assays showed a significantly slower cell migration speed compared to the basal locomotory activity of untreated PC-9 cells. Perhaps more importantly, the highly migratogenic phenotype of PC-9 cells observed in response to the exogenous supplementation with the EMT inducer TGFβ1 was fully prevented in the presence of silibinin meglumine (Fig. 3B).

4. Discussion

Beyond its hepatoprotective effects, the pharmacological activity of silymarin is being revisited due to growing evidence that suggests potential anti-cancer activity. Silibinin was found to exhibit cardioprotective properties during cancer treatments with chemotherapeutic drugs that are known to exert cardiotoxic side effects, such as the anthracycline doxorubicin (Psotova et al., 2002). Orally administered silibinin suppressed the growth of NSCLC A549 xenografts, enhanced therapeutic responses to doxorubicin, and diminished chemoresistance mechanisms via NF-kB modulation (Singh et al., 2004). Moreover, silibinin has also been shown to inhibit NSCLC A549 cell invasion by decreasing the expression of metalloproteinase-2 (MMP-2) and urokinase plasminogen activator (u-PA) (Chu et al., 2004). The anti-invasive effects of silibinin were accompanied by the concomitant inhibition of extracellular signal-regulated kinase (ERK) and AKT activation (Chen et al., 2005), a tumor growth inhibitory mechanism that has been recently confirmed in ovarian cancer cells (Cho et al., 2013). The evidence that suggests silibinin as a possible drug candidate for tumor growth inhibition has been notably reinforced by a landmark study in which the combination of silibinin and the EGFR TKI erlotinib drastically suppressed tumor growth in NSCLC cells that had acquired TKI resistance *via* the EGFR *T790M* mutation (Rho et al., 2010). Although this finding provided a new, unexpected therapeutic avenue for clinical EGFR TKI efficacy management in NSCLC patients, it should be acknowledged that the poor water solubility and low bioavailability of silibinin are expected to severely limit its clinical efficacy. Because the ionization ability of silibinin increases when it is combined with the sorbitol-derived meglumine amino-sugar, in the present study, we decided to use silibinin meglumine as an inexpensive adjuvant strategy with which to administer silymarin to mice that were subcutaneously xenotransplanted with NSCLC human cells and to demonstrate that the water solubility of this formulation is complete and thus no sophisticated methods are required to prepare an orally active silibinin formulation with *in vivo* anti-cancer activity.

This paper provides an initial report of the potent inhibitory effects of the silibinin meglumine formulation on NSCLC cancer growth in an *in vivo* xenograft model that was generated by subcutaneously injecting PC-9 cells into athymic mice. Specifically, we

demonstrate that a 5-week period of oral silibinin-meglumine administration at 100 mg/kg per day is as efficient as the EGFR TKI gefitinib in terms of significant PC-9 tumor xenograft growth inhibition. Importantly, our data demonstrate that mice receiving concomitant silibinin-meglumine and gefitinib treatments show an impressive tumor growth reduction of approximately 75% after 35 days of combined treatment. Because the PC-9 tumor growth inhibition persisted in the combination group even after the drugs were discontinued, these findings suggest that whereas the regrowth of some individual tumors can be observed after a few weeks of single-agent gefitinib treatment (thus mimicking clinical relapses), the concomitant administration of silibinin meglumine appears to impede the regrowth of gefitinib-unresponsive tumors. In this regard, our findings, in which silibinin meglumine treatment efficiently impedes pro-EMT signaling in EGFR-mutant NSCLC cells *in vitro* and *in vivo*, raise the possibility that EMT that arises during gefitinib-resistance development, as observed in EGFR-mutant NSCLC both *in vitro* and *in vivo* (Bryant et al., 2012; Byers et al., 2013; Thomson et al., 2005; Chang et al., 2011; Chung et al., 2011; Coldren et al., 2006; Fuchs et al., 2008; Nurwidya et al., 2012; Suda et al., 2011; Yauch et al., 2005; Zhang et al., 2012, 2013), could be countered by the concomitant presence of silibinin-meglumine. In recent years, the EMT, a traditional phenomenon revealed in embryonic development that is defined by the loss of epithelial characteristics and the acquisition of a mesenchymal phenotype, has been gradually accepted as a pivotal mechanism underlying different aspects of cancer progression, such as metastasis, stem cell traits, and resistance to cancer therapies (Dave et al., 2012; De Craene and Berx, 2013; Kalluri and Weinberg, 2009; Meng and Wu, 2012; Micalizzi et al., 2010; Nieto and Cano, 2012; Scheel and Weinberg, 2012; Singh and Settleman, 2010; Thiery et al., 2009). Indeed, due to the close relationship of EMT to cancer metastasis and drug resistance, targeting EMT or reversing EMT is likely to lead to novel therapeutic approaches for the treatment of human carcinomas including NSCLC. In this regard, elucidating how EMT could be prevented or reversed in NSCLC might enable the development of new strategies aimed at optimizing the efficacy of EGFR TKIs to improve the therapeutic outcome of NSCLC patients because emerging evidence strongly suggests that the mesenchymal phenotype is closely related to the lack of responsiveness to EGFR TKIs. Although the inhibition of EMT can be a critical strategy for delaying or preventing tumor progression after treatment with EGFR TKIs, the reversal of the EMT-driven erlotinib-refractory phenotype is urgently needed to expand the current EMT-targeted therapies. Earlier studies have shown that silibinin reverses EMT by decreasing the levels of key EMT transcription factors, such as SLUG, and increasing the expression levels of E-cadherin in prostate cancer cells (Singh et al., 2008; Wu et al., 2010; Deep et al., 2011). During the preparation of this manuscript, (Mateen et al., 2013) reported that a combination of silibinin and histone deacetylase and DNA methyltransferase inhibitors significantly restored E-cadherin levels in NSCLC cells with epigenetically silenced E-cadherin expression; experiments with NSCLC cells that expressed basal levels of E-cadherin showed that silibinin treatment further increased E-cadherin expression and inhibited the migratory and invasive potential of these cells (Mateen et al., 2013). These findings provide a mechanistic explanation for our discovery that silibinin meglumine treatment efficiently prevents TGFβ1-driven losses of proteins associated with a polarized epithelial phenotype (i.e., E-cadherin) as well as the *de novo* synthesis of proteins associated with the mesenchymal migratory morphology of transitioning cells (e.g., vimentin). Importantly, we have been able to demonstrate the silibinin meglumine's ability to prevent the acquisition of a mesenchymal phenotype *in vivo*, which took place through a molecular mechanism that likely involved the suppression of the overactivation of *TWIST1* and *N-cadherin*, two useful cross-regulated biomarkers for predicting the prognosis of NSCLC (Hui et al., 2013). We also showed that the combination of silibinin meglumine with gefitinib was highly efficacious at preventing the activation of an EMT genetic program in response to observed with single agent gefitinib, suggesting that the alterations in specific EMT-related mRNAs mediated by silibinin meglumine, which led to the reversal of the mesenchymal phenotype, could be a novel approach for the prevention of acquired resistance to gefitinib in NSCLC treatment.

Throughout the duration of the experiment, the mice treated with silibinin-meglumine did not show any gross signs of toxicity or possible adverse effects as assessed by body weight gain (supplementary Fig. 1) and diet consumption profiles. Therefore, our results that demonstrate the strong *in vivo* antitumor efficacy of oral silibinin meglumine administration in combination with gefitinib in PC-9 tumor xenografts in the apparent absence of toxicity might prompt further interest in the use of silibinin-meglumine as a drug modality in EGFR-mutant NSCLC patients. According to the formula proposed for calculating human equivalent dose (HED) by normalizing the body surface area rather than weight (Reagan-Shaw et al., 2008) (e.g., animal dose (mg/kg) × (animal km factor/human km factor)), we found that the corresponding HED for the maximum dose of silibinin meglumine used in our *in vivo* study, which was equivalent to 100 mg/kg mouse body weight, is a human equivalent dose of 8.11 mg/kg. This equates to a 486.49 mg dose of silibinin meglumine for a 60 kg individual, an HED that is likely within the dose range that can be achieved in target cancer tissues (Kidd, 2009).

5. Conclusions

The liposoluble silymarin has been the chief market product (70–80%) of the *S. marianum* extract (Zhao et al., 2006). The remaining solvent is harmful to humans; furthermore, water-insolubility leads to low bioavailability. It is therefore urgent to develop a water-soluble silymarin form for target preparations to produce new breakthroughs in injections, granules, beverages or health food formulations. Meglumine salt, a product from the reaction between silibinin and organic amine, was one of the earliest organic amine silymarin salts that could change silibinin into a water-soluble preparation (Pei et al., 2009). Currently, silibinin meglumine is commercially formulated in tablets or capsules, and patients must ingest several doses per day to maintain effective plasma concentrations (Cao et al., 2012). Therefore, it might be valuable to develop new technologies that can achieve high levels of efficacy and a long-term drug-release pattern to reduce the drug administration frequency. Furthermore, such a delivery system must be safe after either oral or intravenous administration. In this regard, silibinin meglumine has been successfully incorporated into silica nanoparticles to achieve an excellent linear relationship between *in vitro* dissolution and *in vivo* absorption, thus suggesting a promising model for the sustained released of water-soluble silibinin (Cao et al., 2012). Because an oral silibinin formulation with enhanced solubility and stability over a wide pH range will significantly increase cancer treatment convenience and flexibility, our current *in vivo* findings regarding a non-toxic, orally active water-soluble silibinin formulation could certainly accelerate further in-depth preclinical and clinical studies to determine the value of natural agents such as silibinin that can enhance the clinical efficacies of EGFR TKIs in patients with EGFR mutant-NSCLC.

Conflict of Interest

AstraZeneca (Spain) provided partial financial support for the present study via an educational grant to Drs. Javier A. Menendez and Joaquim Bosch-Barrera.

Acknowledgements

This work was supported by a charity collection that was organized by the Fundació Roses Contra el Cáncer (Roses, Girona, Catalonia). This work was supported financially by grants CP05-00090, PI06-0778, and RD06-0020-0028 from the Instituto de Salud Carlos III (Ministerio de Sanidad y Consumo, Fondo de Investigación Sanitaria (FIS), Spain, the Fundación Científica de la Asociación Española Contra el Cáncer (AECC, Spain), and the Ministerio de Ciencia e Innovación (SAF2009-11579 and SAF2012-389134, Plan Nacional de I+D+I, MICINN, Spain). Alejandro Vazquez-Martin received a Sara Borrell postdoctoral contract (CD08/00283) from the Ministerio de Sanidad y Consumo, Fondo de Investigación Sanitaria -FIS-, Spain). Sílvia Cufí received a research fellowship (Formación de Personal Investigador, FPI) from the Ministerio de Ciencia e Innovación (MICINN, Spain). This work was also supported by grants AGL2011-29857-C03-03 (MICINN, Spain), PROMETEO/2012/007 and ACOMP/2013/093 (Generalitat Valenciana), and CIBER (CB12/03/30038, Fisiopatología de la Obesidad y la Nutrición, CIBERobn, Instituto de Salud Carlos III).

Appendix A. Supplementary material

Supplementary data associated with this article can be found, in the online version, at http://dx.doi.org/10.1016/j.fct.2013.07.063.

References

Brinda, B.J., Zhu, H.J., Markowitz, J.S., 2012. A sensitive LC-MS/MS assay for the simultaneous analysis of the major active components of silymarin in human plasma. J. Chromatogr. B Analyt. Technol. Biomed. Life Sci. 902, 1–9.

Bryant, J.L., Britson, J., Balko, J.M., Willian, M., Timmons, R., Frolov, A., Black, E.P., 2012. A microRNA gene expression signature predicts response to erlotinib in epithelial cancer cell lines and targets EMT. Br. J. Cancer 106, 148–156.

Byers, L.A., Diao, L., Wang, J., Saintigny, P., Girard, L., Peyton, M., Shen, L., Fan, Y., Giri, U., Tumula, P.K., Nilsson, M.B., Gudikote, J., Tran, H., Cardnell, R.J., Bearss, D.J., Warner, S.L., Foulks, J.M., Kanner, S.B., Gandhi, V., Krett, N., Rosen, S.T., Kim, E.S., Herbst, R.S., Blumenschein, G.R., Lee, J.J., Lippman, S.M., Ang, K.K., Mills, G.B., Hong, W.K., Weinstein, J.N., Wistuba, I.I., Coombes, K.R., Minna, J.D., Heymach, J.V., 2013. An epithelial-mesenchymal transition (EMT) gene signature predicts resistance to EGFR and PI3K inhibitors and identifies Axl as a therapeutic target for overcoming EGFR inhibitor resistance. Clin. Cancer Res. 19, 279–290.

Calani, L., Brighenti, F., Bruni, R., Del Rio, D., 2012. Absorption and metabolism of milk thistle flavanolignans in humans. Phytomedicine 20, 40–46.

Cao, X., Deng, W.W., Fu, M., Wang, L., Tong, S.S., Wei, Y.W., Xu, Y., Su, W.Y., Xu, X.M., Yu, J.N., 2012. In vitro release and in vitro-in vivo correlation for silybin meglumine incorporated into hollow-type mesoporous silica nanoparticles. Int. J. Nanomedicine 7, 753–762.

Chang, T.H., Tsai, M.F., Su, K.Y., Wu, S.G., Huang, C.P., Yu, S.L., Yu, Y.L., Lan, C.C., Yang, C.H., Lin, S.B., Wu, C.P., Shih, J.Y., Yang, P.C., 2011. Slug confers resistance to the epidermal growth factor receptor tyrosine kinase inhibitor. Am. J. Respir. Crit. Care Med. 183, 1071–1079.

Chen, P.N., Hsieh, Y.S., Chiou, H.L., Chu, S.C., 2005. Silibinin inhibits cell invasion through inactivation of both PI3K-Akt and MAPK signaling pathways. Chem. Biol. Interact. 156, 141–150.

Chinese-State-Drug-Administration, 2002. The Medical Hepatobiliary Fascicule of Chinese Patent Medicine from Local Standard to National Standard. In: C.S.D. Administration. Chinese State Drug Standard. pp. 299–303

Cho, H.J., Suh, D.S., Moon, S.H., Song, Y.J., Yoon, M.S., Park, D.Y., Choi, K.U., Kim, Y.K., Kim, K.H., 2013. Silibinin Inhibits Tumor Growth through Downregulation of Extracellular Signal-Regulated Kinase and Akt in Vitro and in Vivo in Human Ovarian Cancer Cells. J. Agric. Food Chem., 2013. April 18. [Epub ahead of print].

Chu, S.C., Chiou, H.L., Chen, P.N., Yang, S.F., Hsieh, Y.S., 2004. Silibinin inhibits the invasion of human lung cancer cells via decreased productions of urokinase-plasminogen activator and matrix metalloproteinase-2. Mol. Carcinog. 40, 143–149.

Chung, J.H., Rho, J.K., Xu, X., Lee, J.S., Yoon, H.I., Lee, C.T., Choi, Y.J., Kim, H.R., Kim, C.H., Lee, J.C., 2011. Clinical and molecular evidences of epithelial to mesenchymal transition in acquired resistance to EGFR-TKIs. Lung Cancer 73, 176–182.

Coldren, C.D., Helfrich, B.A., Witta, S.E., Sugita, M., Lapadat, R., Zeng, C., Barón, A., Franklin, W.A., Hirsch, F.R., Geraci, M.W., Bunn Jr., P.A., 2006. Baseline gene expression predicts sensitivity to gefitinib in non-small cell lung cancer cell lines. Mol. Cancer Res. 4, 521–528.

Dave, B., Mittal, V., Tan, N.M., Chang, J.C., 2012. Epithelial-mesenchymal transition, cancer stem cells and treatment resistance. Breast Cancer Res. 14, 202.

De Craene, B., Berx, G., 2013. Regulatory networks defining EMT during cancer initiation and progression. Nat. Rev. Cancer 13, 97–110.

de Groot, H., Rauen, U., 1998. Tissue injury by reactive oxygen species and the protective effects of flavonoids. Fundam. Clin. Pharmacol. 12, 249–255.

Deep, G., Gangar, S.C., Agarwal, C., Agarwal, R., 2011. Role of E-cadherin in antimigratory and antiinvasive efficacy of silibinin in prostate cancer cells. Cancer Prev. Res. (Phila) 4, 1222–1232.

Flora, K., Hahn, M., Rosen, H., Benner, K., 1998. Milk thistle (*Silybum marianum*) for the therapy of liver disease. Am. J. Gastroenterol. 93, 139–143.

Fraschini, F., Demartini, G., Esposti, D., 2002. Pharmacology of silymarin. Clin. Drug Invest. 22, 51–65.

Fuchs, B.C., Fujii, T., Dorfman, J.D., Goodwin, J.M., Zhu, A.X., Lanuti, M., Tanabe, K.K., 2008. Epithelial-to-mesenchymal transition and integrin-linked kinase mediate sensitivity to epidermal growth factor receptor inhibition in human hepatoma cells. Cancer Res. 68, 2391–2399.

Halbach, G., Trost, W., 1974. Chemistry and pharmacology of silymarin. Studies on various metabolites of silybin. Arzneimittelforschung 24, 866–867.

He, J., Hou, S.X., Feng, J.F., Cai, B.Q., 2005. Effect of particle size on oral absorption of silymarin-loaded solid lipid nanoparticles. Zhongguo Zhong Yao Za Zhi 30, 1651–1653.

Hui, L., Zhang, S., Dong, X., Tian, D., Cui, Z., Qiu, X., 2013. Prognostic significance of twist and N-cadherin expression in NSCLC. PLoS One 8, e62171.

Javed, S., Kohli, K., Ali, M., 2011. Reassessing bioavailability of silymarin. Altern. Med. Rev. 16, 239–249.

Kalluri, R., Weinberg, R.A., 2009. The basics of epithelial-mesenchymal transition. J. Clin. Invest. 119, 1420–1428.

Kidd, P.M., 2009. Bioavailability and activity of phytosome complexes from botanical polyphenols: the silymarin, curcumin, green tea, and grape seed extracts. Altern. Med. Rev. 14, 226–246.

Kuki, A., Nagy, L., Deák, G., Nagy, M., Zsuga, M., Kéki, S., 2012. Identification of silymarin constituents: an improved HPLC-MS method. Chromatographia 75, 175–180.

Lee, D.Y., Liu, Y., 2003. Molecular structure and stereochemistry of silybin A, silybin B, isosilybin A, and isosilybin B, Isolated from *Silybum marianum* (milk thistle). J. Nat. Prod. 66, 1171–1174.

Liu, F.Z., Yan, K.X., 1996. Study on the beta-CB silymarin. Lishizhen Medicine and Materia Medica Res. 7, 146–147.

Lu, Y.K., JIi, S.Y., Zhong, L., 1999. Effect of silybin-MG on the production of nitric oxide in rat renal tissue induced by cisplatin. J. Dalian Med. Univ. 61, 7–10.

Mateen, S., Raina, K., Agarwal, C., Agarwal, R., 2012. Epigenetic modifications and p21-cyclin B1 nexus in anticancer effect of histone deacetylase inhibitors in combination with silibinin on non-small-cell lung cancer cells. Epigenetics 10, 1161–1172.

Mateen, S., Raina, K., Agarwal, C., Chan, D., Agarwal, R., 2013. Silibinin synergizes with histone deacetylase and DNA methyltransferase inhibitors in upregulating e-cadherin expression together with inhibition of migration and invasion of human non-small cell lung cancer cells. J. Pharmacol. Exp. Ther. 345, 206–214.

Mateen, S., Tyagi, A., Agarwal, C., Singh, R.P., Agarwal, R., 2010. Silibinin inhibits human nonsmall cell lung cancer cell growth through cell-cycle arrest by modulating expression and function of key cell-cycle regulators. Mol. Carcinogenesis 49, 247–258.

Meng, F., Wu, G., 2012. The rejuvenated scenario of epithelial-mesenchymal transition (EMT) and cancer metastasis. Cancer Metastasis Rev. 31, 455–467.

Micalizzi, D.S., Farabaugh, S.M., Ford, H.L., 2010. Epithelial-mesenchymal transition in cancer: parallels between normal development and tumor progression. J. Mammary Gland Biol. Neoplasia 15, 117–134.

Morazzoni, P., Montalbetti, A., Malandrino, S., Pifferi, G., 1993. Comparative pharmacokinetics of silipide and silymarin in rats. Eur. J. Drug Metab. Pharmacokinet. 18, 289–297.

Nakashima, H., Hashimoto, N., Aoyama, D., Kohnoh, T., Sakamoto, K., Kusunose, M., Imaizumi, K., Takeyama, Y., Sato, M., Kawabe, T., Hasegawa, Y., 2012. Involvement of the transcription factor twist in phenotype alteration through epithelial-mesenchymal transition in lung cancer cells. Mol. Carcinog. 51, 400–410.

Nieto, M.A., Cano, A., 2012. The epithelial-mesenchymal transition under control: global programs to regulate epithelial plasticity. Sem. Cancer Biol. 22, 361–368.

Nurwidya, F., Takahashi, F., Murakami, A., Takahashi, K., 2012. Epithelial mesenchymal transition in drug resistance and metastasis of lung cancer. Cancer Res. Treat. 44, 151–156.

Pallier, K., Cessot, A., Côté, J.F., Just, P.A., Cazes, A., Fabre, E., Danel, C., Riquet, M., Devouassoux-Shisheboran, M., Ansieau, S., Puisieux, A., Laurent-Puig, P., Blons, H., 2012. TWIST1 a new determinant of epithelial to mesenchymal transition in EGFR mutated lung adenocarcinoma. PLoS One 7, e29954.

Pei, W., Chen, Y.-p., Li, J., 2009. Progress in research and application of silymarin. Med. Aromat. Plant Sci. Biotechnol. 3, 1–8.

Psotova, J., Chlopcikova, S., Grambal, F., Simanek, V., Ulrichova, J., 2002. Influence of silymarin and its flavonolignans on doxorubicin-iron induced lipid peroxidation in rat heart microsomes and mitochondria in comparison with quercetin. Phytother. Res. 16 (Suppl 1), S63–S67.

Reagan-Shaw, S., Nihal, M., Ahmad, N., 2008. Dose translation from animal to human studies revisited. FASEB J. 22, 659–661.

Rho, J.K., Choi, Y.J., Jeon, B.S., Choi, S.J., Cheon, G.J., Woo, S.K., Kim, H.R., Kim, C.H., Choi, C.M., Lee, J.C., 2010. Combined treatment with silibinin and epidermal growth factor receptor tyrosine kinase inhibitors overcomes drug resistance caused by T790M mutation. Mol. Cancer Ther. 9, 3233–3243.

Scheel, C., Weinberg, R.A., 2012. Cancer stem cells and epithelial-mesenchymal transition: concepts and molecular links. Semin. Cancer Biol. 22, 396–403.
Singh, A., Settleman, J., 2010. EMT, cancer stem cells and drug resistance: an emerging axis of evil in the war on cancer. Oncogene 29, 4741–4751.
Singh, R.P., Mallikarjuna, G.U., Sharma, G., Dhanalakshmi, S., Tyagi, A.K., Chan, D.C., Agarwal, C., Agarwal, R., 2004. Oral silibinin inhibits lung tumor growth in athymic nude mice and forms a novel chemocombination with doxorubicin targeting nuclear factor kappaB-mediated inducible chemoresistance. Clin. Cancer Res. 10, 8641–8647.
Singh, R.P., Raina, K., Sharma, G., Agarwal, R., 2008. Silibinin inhibits established prostate tumor growth, progression, invasion, and metastasis and suppresses tumor angiogenesis and epithelial-mesenchymal transition in transgenic adenocarcinoma of the mouse prostate model mice. Clin. Cancer Res. 14, 7773–7780.
Suda, K., Tomizawa, K., Fujii, M., Murakami, H., Osada, H., Maehara, Y., Yatabe, Y., Sekido, Y., Mitsudomi, T., 2011. Epithelial to mesenchymal transition in an epidermal growth factor receptor-mutant lung cancer cell line with acquired resistance to erlotinib. J. Thorac. Oncol. 6, 1152–1161.
Tang, X.Z., Hou, S.X., He, Y.J., Wang, B.N., 2001. Preparation and in vitro evaluation of silymarin solid dispersions and complexation. West China J. Pham. Sci. 16, 193–195.
Thiery, J.P., Acloque, H., Huang, R.Y., Nieto, M.A., 2009. Epithelial-mesenchymal transitions in development and disease. Cell 139, 871–890.
Thomson, S., Buck, E., Petti, F., Griffin, G., Brown, E., Ramnarine, N., Iwata, K.K., Gibson, N., Haley, J.D., 2005. Epithelial to mesenchymal transition is a determinant of sensitivity of non-small-cell lung carcinoma cell lines and xenografts to epidermal growth factor receptor inhibition. Cancer Res. 65, 9455–9462.
Wang, K., Zhang, H., Shen, L., Du, Q., Li, J., 2010. Rapid separation and characterization of active flavonolignans of *Silybum marianum* by ultra-performance liquid chromatography coupled with electrospray tandem mass spectrometry. J. Pharm. Biomed. Anal. 53, 1053–1057.
Wu, K., Zeng, J., Li, L., Fan, J., Zhang, D., Xue, Y., Zhu, G., Yang, L., Wang, X., He, D., 2010. Silibinin reverses epithelial-to-mesenchymal transition in metastatic prostate cancer cells by targeting transcription factors. Oncol. Rep. 23, 1545–1552.
Xiao, Y.Y., Song, Y.M., Chen, Z.P., Ping, Q.N., 2005. Preparation of silymarin proliposomes and its pharmacokinetics in rats. Yao Xue Xue Bao 40, 758–763.
Yauch, R.L., Januario, T., Eberhard, D.A., Cavet, G., Zhu, W., Fu, L., Pham, T.Q., Soriano, R., Stinson, J., Seshagiri, S., Modrusan, Z., Lin, C.Y., O'Neill, V., Amler, L.C., 2005. Epithelial versus mesenchymal phenotype determines in vitro sensitivity and predicts clinical activity of erlotinib in lung cancer patients. Clin. Cancer Res. 11, 8686–8698.
Yu, J.N., Xu, X.M., Zhu, Y., Gao, H., 2003. Determination of concentration and encapsulation efficiency of silybin liposomes. Zhongguo Zhong Yao Za Zhi 28, 1027–1030.
Zhang, X., Liu, G., Kang, Y., Dong, Z., Qian, Q., Ma, X., 2013. N-Cadherin expression is associated with acquisition of EMT phenotype and with enhanced invasion in erlotinib-resistant lung cancer cell lines. PLoS One 8, e57692.
Zhang, Z., Lee, J.C., Lin, L., Olivas, V., Au, V., LaFramboise, T., Abdel-Rahman, M., Wang, X., Levine, A.D., Rho, J.K., Choi, Y.J., Choi, C.M., Kim, S.W., Jang, S.J., Park, Y.S., Kim, W.S., Lee, D.H., Lee, J.S., Miller, V.A., Arcila, M., Ladanyi, M., Moonsamy, P., Sawyers, C., Boggon, T.J., Ma, P.C., Costa, C., Taron, M., Rosell, R., Halmos, B., Bivona, T.G., 2012. Activation of the AXL kinase causes resistance to EGFR-targeted therapy in lung cancer. Nat. Genet. 44, 852–860.
Zhao, X.Y., Wang, B.E., Wang, T.L., Li, X.M., 2006. Inhibitory effects of silymarin on hepatic fibrosis induced by dimethylnitrosamine: experiment with rats. Zhonghua Yi Xue Za Zhi 86, 2563–2566.